

DIFFERENTIAL MODE DELAY (DMD) FOR MULTIMODE FIBER TYPES AND ITS RELATIONSHIP TO MEASURED PERFORMANCE

Rick Pimpinella and Al Brunsting
Fiber Research Department

Panduit Corp., Orland Park, IL 60427

Abstract – With the introduction of Vertical Cavity Surface Emitting Lasers (VCSEL's) used with multimode fiber (MMF), Differential Mode Delay (DMD), modal interference effects and the influence of connector interfaces are found to reduce the observed bandwidth of multimode fibers (MMF's). In this study the performance of three example MMF's is characterized by measuring DMD and is compared to Bit Error Rate (BER) measurements on the same three fibers. Fiber length is also considered. Controlling the spatial locations of the launch pulses, we develop methods aimed to certify the performance of optical fiber for 10Gb/s Ethernet. The source for these measurements was an 850nm VCSEL.

©2005 Optical Society of America

OCIS codes: (060.0060) Fiber optics and optical communications, (060.2270) Fiber characterization, (060.2300) Fiber measurements.

1. INTRODUCTION

It is now clear that of the bandwidth of a significant fraction of legacy MMF and laser-based transceivers (such as VCSELs) does not support data rates up to 10-Gb/s and lengths of 300-m. This is due mostly to the design of these fibers which were optimized for lower bit rates and light emitting diode (LED) transmitters. The fiber cores were designed to be overfilled and thereby the LEDs couple optical power into all, or nearly all, of the fiber modes. However, when the small spot from a VCSEL illuminates a fiber core, optical power is coupled into a small fraction of the available modes (several hundred). The actual supported bandwidth of installed legacy MMF, using laser-based transceivers, can be (and usually is) unpredictable.

New laser optimized MMF supports these higher data rates up to 300-m, specified as OM-3 by ISO 11801 and 850-nm Laser Optimized 50 micron (850 LO 50) by TIA. The only accepted way to characterize these high bandwidth MMF's is with DMD measurements. See, for example, ref. [1].

This paper will describe such DMD measurements and relate the results to measured MMF performance as

determined by the fiber's bit error rate (BER). Optical pulses are launched into the MMF core at precisely controlled offsets from the fiber axis and have fast rise and fall times, referred to as restricted launch conditions, compared to overfilled launched conditions using an LED. Emerging pulses from the MMF are measured and saved in the time domain (voltage vs. time) by a fast received and data storage device. We will show that the DMD measurements correlate with MMF length, fiber type, and the corresponding BER.

2. PERFORMANCE OF MULTIMODE FIBERS (MMF)

2.1 Refractive index profile

The refractive index of the MMF core varies as a function of distance from the core axis (refractive index profile). The specific shape of the refractive index profile in the core has a significant effect on the distribution of the guided optical power in the fiber. But more importantly, the index profile profoundly influences the velocities of the various propagating modes, which results in dispersion. A parabolic index distribution nearly equalizes the group velocities of the propagating modes and fiber manufacturers strive to optimize the specific index distribution to minimize dispersion.

A general refractive-index profile is given by Eq. (1).

$$n(r) = \begin{cases} n_{core} \cdot [1 - 2 \cdot \Delta \cdot (r/r_{core})^\alpha]^{1/2} & r < r_{core} \\ n_{clad} & r \geq r_{core} \end{cases} \quad (1)$$

where Δ is the relative refractive index difference between core and cladding and given by $\Delta = 0.5(n_{core}^2 - n_{clad}^2)/n_{core}^2$. The power law parameter is α .

A set of perturbed refractive index profiles, relative to Equation (1), has been proposed to describe MMF that is representative of installed fiber [2]. Even though these perturbations were used for 1300nm and a core diameter of 62.5 μ m a similar set of perturbations can be generated for 850nm and a core diameter of 50.0 μ m to describe those corresponding applications. In ref. 1 the effects of perturbed refractive index profiles on DMD-type results were simulated and shown to be significantly dependent on the refractive index profile and amount of offset launch [2].

DMD measurements, described in Section 3, are similar to these offset launch conditions.

2.2 Vertical Cavity Surface Emitting lasers (VCSELs).

In MMF systems the optical source is traditionally an LED and depending on the material system, operates at either long or short wavelengths (1310nm or 850nm respectively). Unlike Fabry-Perot (FP) and Distributed Feedback (DFB) lasers, LED's are mainly surface emitting devices, having a broad spectral output with large numerical aperture (NA). The large core diameters in MMF (50 μ m, 62.5 μ m and larger) are designed to efficiently couple the LED output power. The LED output overfills the MMF core resulting in an Overfilled Launch (OFL) condition. For an OFL condition the performance of MMF is limited to relatively low bit rates (< 650Mb/s) and, modal dispersion is relatively well behaved.

State-of-the-art high-speed multimode systems such as 10Gigabit Ethernet (10GbE) use newer devices known as VCSEL's. They, like LED's, are surface emitting devices; however, the internal structure of the VCSEL comprises a layer of multiple quantum wells between Bragg Reflectors forming a laser cavity. Hence, although the device is a surface emitter, the output of the VCSEL is similar to that of the more traditional edge-emitting laser. The light emission of the VCSEL is from a single longitudinal mode, although multiple transverse modes with slightly different wavelengths are supported due to the lateral cavity diameter.

Whereas edge-emitting lasers couple few longitudinal modes into single-mode fiber (SMF) and LED's couple large numbers of modes uniformly across the core of the MMF, VCSEL's couple a few transverse modes into a large core MMF in an under-filled launch condition. These

differences in modal output in combination with the optical properties of MMF result in an observed modified behavior for VCSEL signal propagation. For 10GbE systems, the dispersion and interference effects acting on the propagating modes can significantly degrade signal performance, thereby limiting the maximum transmission distances to a few hundred meters. The dispersion and interference effects result in several optical power penalties that reduce the system's overall optical power budget.

2.3 Bit error rate (BER)

Flawless propagation of bits of data through the fiber link is the ultimate design goal of the MMF in that optical link. For our purposes there are two basic measures of this transport performance: (1) the number of bit errors compared to the total number of bits transmitted (BER) per unit time and (2) the speed of the bits passing through the fiber (data rate in bits/sec). Here we will focus on BER.

In Fig. 1 consider digital pulses (bits) being launched into a MMF, represented by "initial pulses". The mean optical power of the (zero, one) bit is (p_0, p_1), W . There is noise on these pulses, p_{noise} . After the pulses have propagated through the MMF they suffer distortions due to differential mode delay and other effects, represented by "final pulses". Additional noise is present in the final pulses.

The difference between p_1 and p_0 for the (initial, final) pulses is ($OMA_{initial}, OMA_{final}$) or optical modulation amplitude. There are two bimodal distributions of optical powers for both the p_1 and p_0 pulses, shown on the right side of Fig. 1. The logic of the associated circuitry is programmed to decide if a given propagated pulse is a 1 or a 0. A comparison is made between the detected optical power of a given pulse within a given time window with a given power threshold, p_{TH} . If a given pulse (bit) starts as a

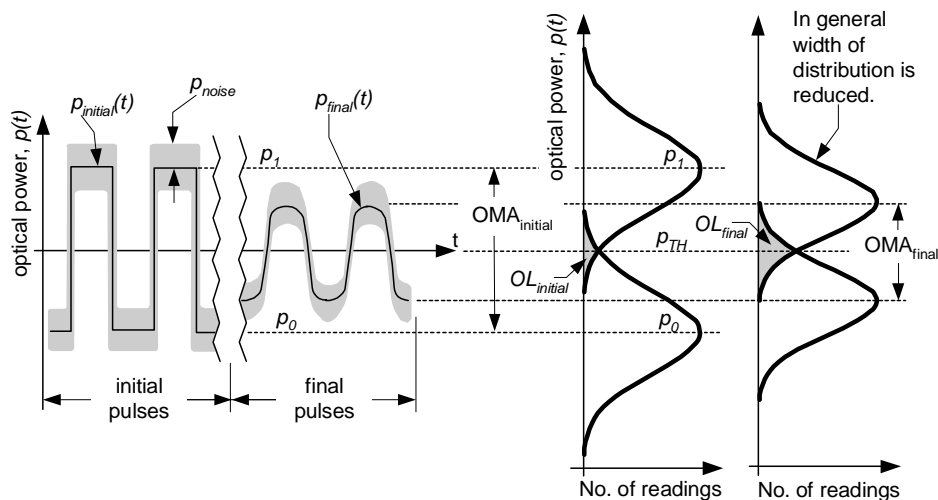


Fig. 1. Explanation of bit error rate (BER). Digital pulses are launched into the multimode fiber (MMF) under test and undergo distortions that result in bit errors. See the text for an explanation of these symbols.

0 and falls above p_{TH} , that bit will be erroneously recorded as a 1. A similar error occurs for a starting 1 bit which falls below p_{TH} . Those bit errors are presented as the gray overlap areas, $OL_{initial}$ and OL_{final} .

The final bit error rate is then the ratio of the final overlap area, OL_{final} , to the total area of the bimodal distribution on the right side of Fig. 1. To reduce the final BER it can be seen that OMA_{final} must be increased and/or p_{noise} must be decreased.

If the data sequence contains consecutive identical digits (case A), then the BER may change compared to alternating digits (0's and 1's, case B). This is because case A may contain significant low-frequency components compared to case B.

3. DIFFERENTIAL MODE DELAY (DMD)

In addition to BER another way to characterize MMF is to measure DMD. A spatially small (compared to the MMF core) and temporally short optical pulse is launched in the core of the MMF end face that is under test. At the output end face the resulting signal is measured [3 - 5]. This measurement is repeated, starting at the axis of the MMF core and moving outward to the core/cladding interface [1]. See Fig. 2 (not scaled and illustrates only the principle). Due to the cylindrical symmetry of the fiber this linear scan responds to many of the MMF modal structures. The launching spot can originate from a single mode fiber (or equivalent). There are additional requirements for the detection system and methods [1].

For a given offset launch only a weighted subset of all the possible mode groups is excited in the MMF. At the next offset launch location in the DMD measurement sequence a different weighted subset of mode groups is excited. In the full sequence of a DMD measurement all the mode groups are excited, according to the weights for each offset location. The different mode groups will, in general, have different propagation times as discussed in Section 2.1, illustrated in Fig. 2 (right-hand plot). Two times are measured, t_{fast} and t_{slow} , determined by the time of 25% of

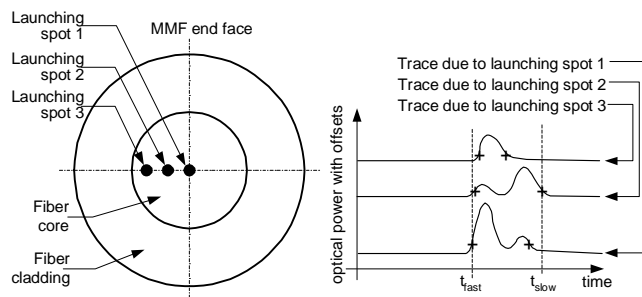


Fig. 2. End face of a MMF, showing three idealized launching spots into the core and an idealized and resulting DMD plot. Leading and trailing edge times (25%) threshold are identified with a “+”.

the pulse maximum of the leading edge of the fastest pulse and 25% of the pulse maximum of the trailing edge of the slowest pulse in this sequence (see Fig. 2).

If all the pulses in the DMD sequence are temporally aligned; then we expect that arrival time of each pulse, propagated by a distribution of mode groups, will be nearly the same from pulse to pulse. This condition translates into lower noise (lower temporal jitter) and a smaller BER (improves). See Fig. 1. Conversely, as the temporal misalignment increases in the DMD sequence, the temporal jitter increases, and the BER increases (becomes worse).

To measure DMD consider the difference between t_{fast} and t_{slow} , which is comprised of DMD (due only to the fiber), the launch optical pulse, and the chromatic dispersion [in ps/(m*km)]. See ref. [1].

4. MEASUREMENTS OF DMD AND MMF PERFORMANCE

4.1 Materials and methods for DMD measurements

The layout of Fig. 3 was used to make DMD measurements. A VCSEL source is embedded in a commercially available XFP transceiver, powered by an evaluation board. Voltage pulses from the pulse generator are differentially supplied to the evaluation board and in response the VCSEL generates optical pulses. The pulse width, period, delay, amplitude, and voltage offsets are all controlled from the pulse generator.

Optical pulses at 850nm are launched into SMF from the VCSEL, resulting in an approximately 18dB signal attenuation, compared to MMF. The launch SMF is positioned to better than 0.5μm accuracy and repeatability by the x-y-z precision location control and the bare fiber

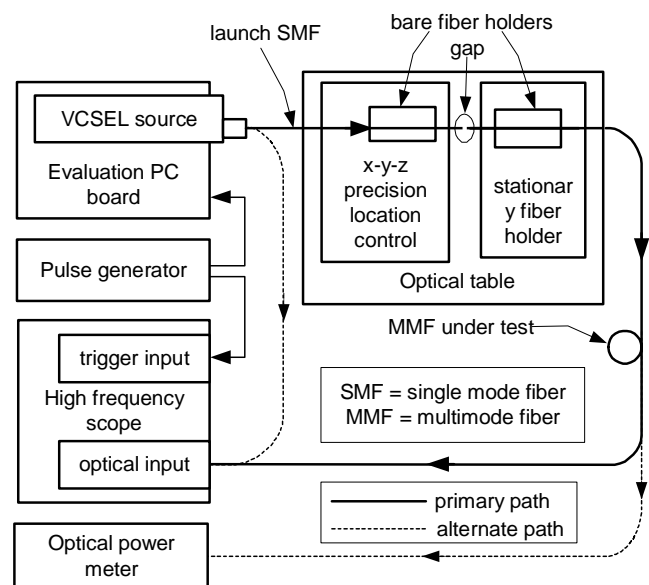


Fig. 3. Summary of the experimental layout.

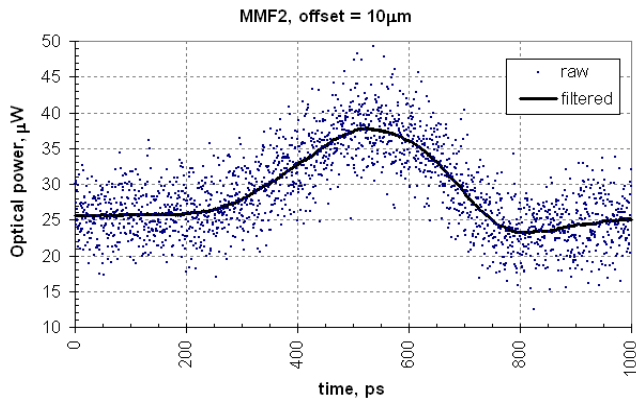


Fig. 4. An example of the digital filtering used for the DMD measurements.

holder. The MMF under test is located with a bare fiber holder mounted on a stationary fiber holder. The gap (less than $10\mu\text{m}$) between the two fiber end faces is where the DMD offset distances are defined. The axis of the SMF output beam is perpendicular to the end face of the MMF to within 1.0° .

Positioning the axis of the SMF congruently with the axis of the MMF requires a detailed procedure (see “Launching spot 1” in Fig. 2). A coarse location is first determined by finding the (horizontal, vertical) edges (x, y) using the optical power meter and the x - y - z precision location control. Based on this estimate of $x = 0$ and $y = 0$, a matrix of measurements is taken with a step size of $5.0\mu\text{m}$ for both x and y directions. Numerical methods are used to weight

the elements in this array (based on optical power, μW) to determine an accurate measurement of $x = 0$ and $y = 0$.

The raw signal from the optical input of the high frequency scope was noisy. Mainly this was due to the low coupling efficiency of the VCSEL into the SMF as mentioned above. Digital filtering was used to reduce much of this noise. An example is shown in Fig. 4. For each interior point of 4096 raw points the optical power was averaged over a window of 200 consecutive points, centered on the raw point. Near the boundaries the averaging was asymmetric and included only those points within the overall time range. For that portion of the filtered optical power that was beyond the range of each pulse, the background structure was deleted and set to zero. The results were thus uncontaminated by background.

Methods from ref. [1] were used to determine DMD in the time domain and are summarized here. The launch SMF was positioned at offset launch locations of $x = 0, 2, \dots, 24\mu\text{m}$ and $y = 0\mu\text{m}$. At each location raw optical pulses from the MMF under test were captured by the scope (see Fig. 3). After digital filtering (Fig. 4) the time locations of 25% of the maximum optical power of each pulse were determined, marked by '+'s in Fig. 5. From the complete set of '+'s the left most '+' and the right-most '+' were determined and are indicated by thicker dashed lines in Fig. 5. This difference defines the time between the leading edge of the fastest resultant pulse and the trailing edge of the slowest resultant pulse. The pulse width due only to the

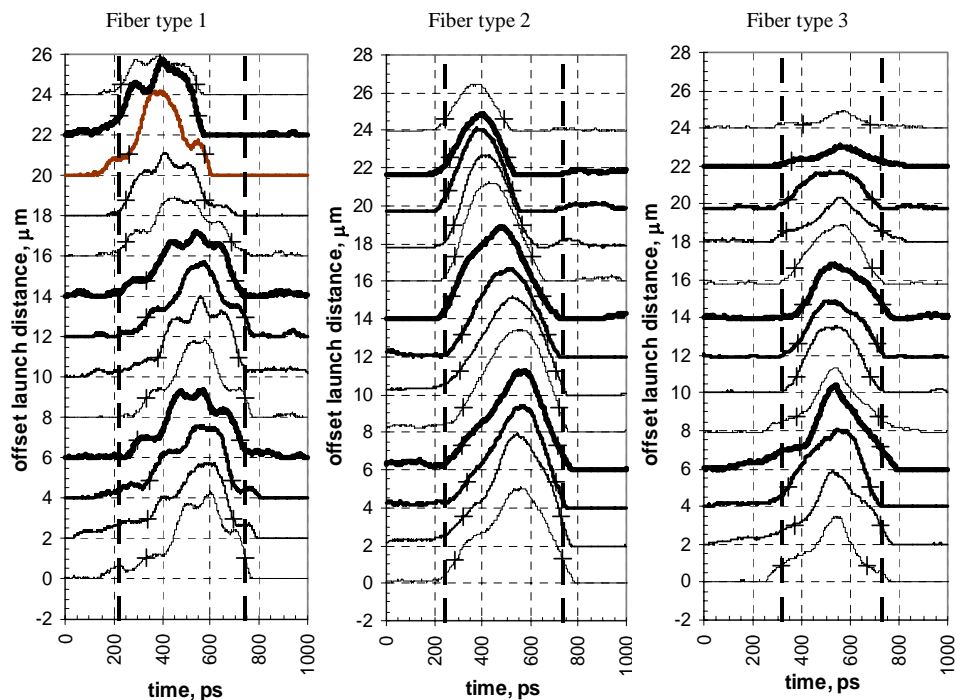


Fig. 5. DMD measurements for the three types of fiber. See the text for details.

fiber can be determined by subtracting the width of the launch pulse from this resultant difference. The pulse width due only to the fiber per unit length, DMD in units of ps/m, is given as follows: [(time distance between these two dashed lines) – (time between corresponding launch pulse points)] / (fiber length). For example, for Fiber type 1 (left-most “+” – right-most “+”) = 525ps. The time between the 25% maximum points of the launch pulse is 229ps. The fiber length is 2438m so that DMD = (525ps-229ps)/2438m = 0.121ps/m.

Longer fiber lengths are typically used for these types of DMD measurements. The lengths used in this study were chosen to balance our requirements for sensitivity to the various DMD pulse delays and our corresponding BER measurements.

4.2 Methods for MMF bandwidth measurements

Following the notation of ref. [1] (Sections 6.2.1 and 6.2.2), let $U(r_j, t_k)$ be the digitally filtered output pulse where U is optical power (in units of Watts), r_j ($j = 1, 2, \dots, M$) are the M offset distances (μm) between the axis of the launch SMF and the axis of the MMF under test (see Fig. 3), and t_k ($k = 1, 2, \dots, N$) are the N discrete times (sec). Note that $U(r_j, t_k)$ is in the time domain. For simplicity here let $W(r_j)$ be the mean of the 10 VCSEL weighting factors, given in Annex D of ref. [1], simulating a typical VCSEL. This method can be readily expanded to include the full set of weighting factors.

A resultant output temporal response function, $P_0(t_k)$, simulates all significant mode groups that are simulated by the typical VCSEL (through the W values) and the MMF under test (through the U values).

$$P_0(t_k) = \sum_{j=1}^M W(r_j) \cdot U(r_j, t_k) \quad (2)$$

Also in the time domain let $R(t_k)$ be the reference pulse that is launched into the MMF under test. This is measured and filtered in the same manner as the $U(r_j, t_k)$ values. In Fig. 3 note the alternate path directly from the VCSEL source to the optical input of the scope to allow an unfiltered measurement of $R(t_k)$.

To represent our VCSEL we took the mean of these matrix elements at each offset distance to weight our results, using $W(r_j)$, ($j = 1, 2, \dots, M$). Summing over all M offsets as described in Eq. 2, gave a resultant pulse in the time domain ($N = 4096$ values in units of Watts vs. ps) for each of the three MMF types. Convert $P_0(t_k)$ in the time domain to the frequency domain using Eq. (3):

$$p_0(f_k) = FT\{P_0(t)\} \quad (3)$$

Here discrete $p_0(f_k)$ values are the N Fourier transform elements of the P_0 values, given in Eq. (2), where $k = 1, 2, \dots, N$ and where f_k are the N frequencies. The Fourier transform function, $FT\{\dots\}$, can be computed in Microsoft® Excel with the Fourier Analysis tool, for example. In Eq. (3) the subscript k was deleted from the time, t , dependency to indicate that all the $P_0(t)$ values are used to calculate each $p_0(f_k)$ value. The magnitude of each complex element within the array of N Fourier transform values is squared to give each $p_0(f_k)$ value to convert from electrical to optical power (e.g., squaring the IMABS(...) function in Excel where the arguments are the elements of the $FT\{\dots\}$ array).

The relationship between time and frequency is

$$\Delta f = 1/(N \cdot \Delta t) \quad (4)$$

where Δt is the time step size (in sec) between the successive N times, t_k , and Δf is the corresponding frequency step size (in Hz) between the successive N frequencies, f_k .

Similarly the reference pulse in the time domain is converted to the frequency domain as given in Eq. (5).

$$r(f_k) = FT\{R(t)\} \quad (5)$$

From the Convolution theorem [6, 7] we have

$$p_0(f_k) = r(f_k) \cdot h(f_k) \quad (6)$$

where $h(f_k)$ is the fiber frequency response, also called the fiber transfer function. This implies that the resultant function, p_0 , is comprised only of the reference pulse, r , and the fiber frequency response, h . The effects due to the connectors and other sources that may affect p_0 are ignored here.

From Eqs. (2) and (3) and the associated measurements the $p_0(f_k)$ values are determined. Using Eq. (5) and its associated measurements the $r(f_k)$ values are determined so that the $h(f_k)$ values can be found from Eq. (6):

$$h(f_k) = p_0(f_k)/r(f_k) \quad (7)$$

The normalized functions for $p_0(f_k)$, $r(f_k)$, and $h(f_k)$ [$p_0(f_k)/p_0(f_1)$, $r(f_k)/r(f_1)$, and $h(f_k)/h(f_1)$] are plotted in Fig. 6. The effective modal bandwidth (EMBc) is found by locating that frequency, f_b , where $h(f_k)$ is 1.5 dB down from the zero frequency, f_1 . The EMBc frequency, f_c , is given by $f_c = 1.414 \cdot f_b$. In practice f_b must be found by interpolation within the $h(f_k)$ array, e.g., a linear interpolation. EMBc typically has units of MHz·km. This means that f_c , in Hz, is to be multiplied by the length of the MMF under test in km and divided by 10^6 Hz/MHz.

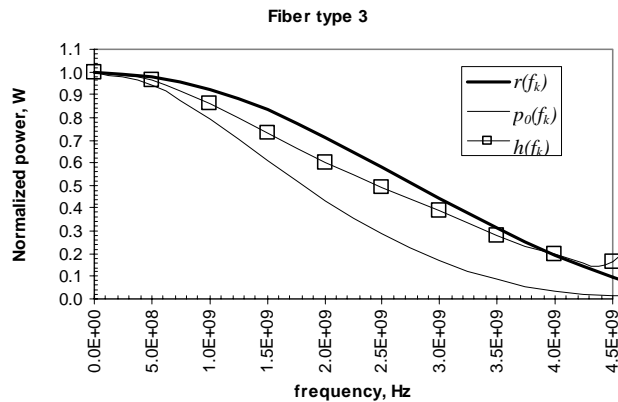


Fig. 6. An example of the three kinds of frequency responses, described in Section 4.2

4.3 Materials and methods for BER measurements

To characterize the optical fibers under test for 10Gb/s Ethernet performance we configured a test and procedure to emulate a 10GBASE-S Ethernet link. The method employs a Bit Error Rate Test (BERT) system to simulate the optical transmitter and receiver and to measure the link performance in terms of bit error rate. The BERT is programmed to take repetitive measurements over extended periods of time. Modal interference effects in the optical link are minimized by eliminating unnecessary modal losses.

The fiber under test is connected to the BERT using two patch cords with their cladding modes suppressed. The Bit Error Rate Test configuration is shown in Fig. 7 where TP refers to test point and (Tx, Rx) refer to optical (transmit, receive) functions. A pattern generator drives the VCSEL transmitter. The output power levels of the transmitted signal were compliant to IEEE 802.3ae [8].

The required performance for a 10GbE system is a

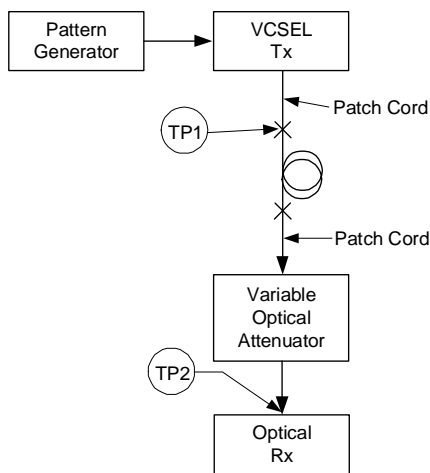


Fig. 7. Bit Error Rate Test Configuration.

specified BER for a minimum receiver power. We characterize the performance of the fiber under test by measuring the BER as a function of receiver average power. The input power to the optical receiver is incrementally reduced by means of an external variable optical attenuator (VOA). For compliance we have confirmed that our 50/125 μ m MMF under test performs to a maximum operating range. For reference, a baseline BER curve is routinely generated for a reference MMF.

For the reference MMF we achieve a specified BER for an average optical receiver power that exceeds the minimum system requirement. It is important to note that performance is highly dependant on the characteristics of the transmitter output pulse, which has been adjusted to meet the requirements. It was observed that seemingly small changes in output launch conditions have large measurable effects on BER performance.

4.4 Results

Using these methods to determine DMD in the time domain, bandwidth, and BER; three distinct fiber types were evaluated. All had core diameters of 50 μ m. Type 1 was laser optimized for 10GbE data rates. An optical time domain reflectometer (OTDR) measurement of fiber length yielded 2438.4m for the DMD measurements. Type 2 was not laser optimized for 10GbE. Its OTDR length was 1019.1m. And Type 3 was laser optimized for 10GbE and had an OTDR length of 1016.1m. A summary of those measurements, including digital filtering, is shown in Fig. 5.

5. DISCUSSION AND CONCLUSIONS

From Fig. 4 it is clear that digital filtering is required to significantly reduce the high frequency component of the noise in the raw measurements. Smooth curves are required to measure DMD where the leading and trailing edges of the slowest and fastest points are analyzed to determine t_{fast} and t_{slow} .

In Fig. 5 we see that the noise is greater for Fiber type 1 than for either type 2 or type 3. This is due to the length of type 1, 2438.4m for the DMD measurements while type 2 was 1019.1m and type 3 was 1016.1m. Comparing Fiber type 2 with Fiber type 3 in Fig. 5, we see that the pulses for

Fiber type 3 line-up nearly perfectly, corresponding to a small DMD for Fiber type 3. The pulses for Fiber type 2 are clearly displaced from each other as a function of offset launch distance, corresponding to clearly not having 10GbE performance at 300m as shown in Fig. 8 (discussed below).

Each of the three fiber types was terminated with connectors such that the total fiber length was 300m. BER measurements were made on all three fiber types and on control and baseline samples. Under automatic control all

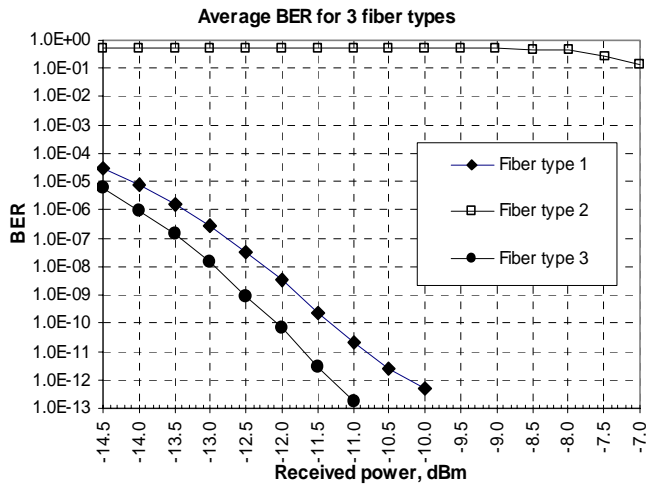


Fig. 8. BER measurements for 3 fiber types. The two curves with solid markers meet the requirements for 10GbE.

results were acquired and subsequently analyzed and plotted (see Fig. 8).

The results are summarized in Table 1 where it is seen that for smaller DMD results (ps/m) we have higher bandwidths (MHz km). Within the MMF under test if the pulses that propagate within the available modal groups all arrive at the scope at nearly the same time are indicated by small DMD values which translate into higher bandwidth capacity. Our results are consistent with this interpretation. The last column compares our measured results with the standard [6] which requires that the MMF transmit data at 10Gbits/s with $BER \leq 10^{-12}$ and received power ≤ -9.9 dBm. Fiber types 1 and 3 pass this requirement but Fiber type 2 does not.

For Fiber type 2 the BER measurement was much different that the BER measurement for the other two fiber types (see Fig. 8). This is consistent with the measured DMD result for Fiber type 2 that is larger than the other two fiber types and the measured bandwidth for Fiber type 2 that is smaller than the other two fiber types.

Comparing the BER results for Fiber types 1 and 3, both of

Table 1. Comparisons of measured DMD, measured bandwidth, and BER for three types of MMF's.

MMF length, type	DMD meas. m	meas. DMD ps/m	meas. bandwidth MHz km	BER length, m	At BER = 10^{-12} , received power, dBm
1	2438	0.121	2830	300	-10.2
2	1019	0.254	1404	300	No signal detected.
3	1619	0.114	2451	300	-11.3

which satisfy the 10GbE requirements, we see that the correlation with measured DMD and measured bandwidth is not perfect. From our experience BER results are sensitive to connector types and blemishes at the connector interfaces, which translate into mode selective losses within the fiber link. We suspect this cause for this type of disagreement.

Generally, we can conclude that there is a less than perfect correlation between BER and measured DMD and bandwidth. DMD measurements mostly depend on modal dispersion but are not so responsive to other causes that limit bandwidth (e.g., inter-symbol interferences). On the other hand, BER is a realistic measurement of bandwidth that includes most, if not all, causes of bandwidth limitations. For the end customer the performance of the fiber link is most importantly determined by BER and data rate.

6. ACKNOWLEDGMENTS

The contributions of Bo Wang are acknowledged who prepared many of the samples and took the BER measurements. Manho Chung also is acknowledged for preparing other samples for the DMD measurements. Ken Reeder arranged for the availability of several of the samples. A discussion with John S. Abbott, Corning Inc., was very helpful.

7. REFERENCES

- [1] "FOTP-220: Differential Mode Delay Measurement of Multimode Fiber in the Time Domain," *TIA/EIA Standards Document*, TIA/EIA 455-220-A, (January 2003).
- [2] M. Webster, L. Raddatz, I. H. White, and D. G. Cunningham, "A statistical Analysis of Conditioned Launch for Gigabit Ethernet Links Using Multimode Fiber", *J. Lightwave Technol.*, **17**, 1532 – 1541 (1999).
- [3] L. Raddatz, I. H. White, D. G. Cunningham, M. C. Nowell, "An experimental and theoretical study of the offset launch technique for the enhancement of the bandwidth of multimode fiber links", *J. Lightwave Technol.*, **16**, 324 – 331 (1998).
- [4] S. E. Golowich, W. A. Reed, "Technique for measuring modal power distribution between an optical source and a multimode fiber", U.S. Pat. 6,788,397, (2004).
- [5] J. B. Schlager and D. L. Franzen, *NIST Symposium on Optical Fiber Measurements*, PP. 127 – 130, (1998).
- [6] J. B. Thomas, "An Introduction to Statistical Communication Theory," New York: Wiley, 1969, p. 143.
- [7] W. H. Press, et al., "Numerical Recipes: The Art of Scientific Computing," Cambridge, UK: Cambridge University Press, 1986, p. 383.
- [8] IEEE 802.3ae – 2002, Part 3: Carrier Sense Multiple Access with Collision Detection (CSMA/CD) Access Method and Physical Layer Specifications (2002).